Sample Site Description

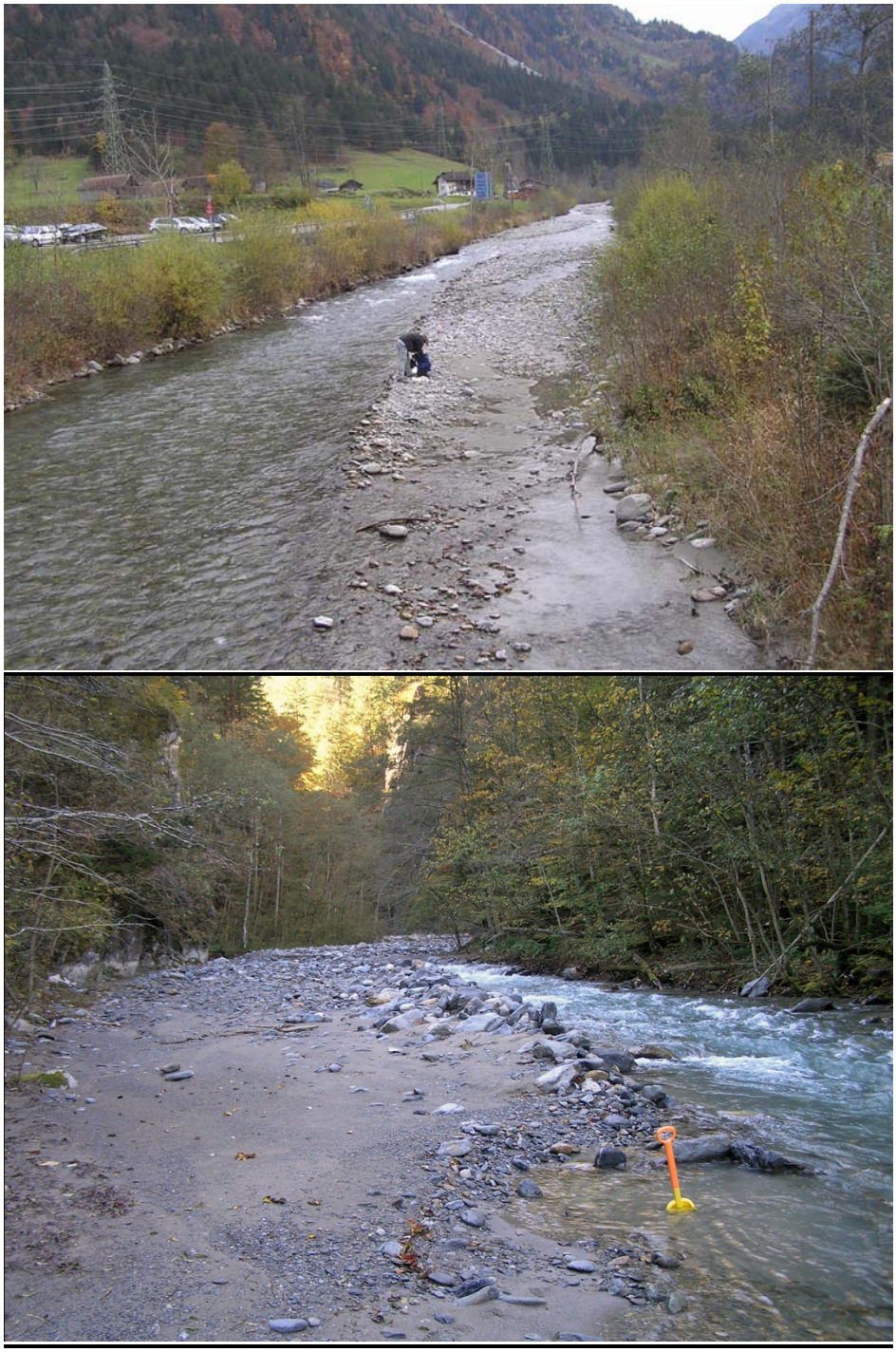

Figure DR1. Aare sampling sites AI (upper picture; October 2008) and site AI2 (lower picture; October 2010). Site AI2, which is 1.5 km upstream of AI (see Fig. 1, main text) was chosen after earthworks at

site AI in late summer 2010. The bar at site AI, made of gravel and sand, has been located in the centre of the modern stream in a relatively stable position. Although the channel is man-made confined at the sampling site, the natural condition starts at the end of the visible part of the channel in the picture (~500 m upstream). Sample site AI2 is a lateral bar made of cobbles, gravels and sand, in a natural gorge-confined channel.

The Spreitlaui Debris-Flow Torrent

We supply a map of the Spreitlaui debris-flow torrent to emphasize on the different regions and sources affected during the 2009 and 2010 debris-flow events. Drainages have been mapped by measuring the concavity perpendicular to the flow direction from a DEM. A threshold value was set qualitatively, to provide a good representation of channel structures in the landscape. This is an appropriate technique to extract channels in DEMs representing formerly glaciated landscapes where critical slope-area thresholds do not play a large role for channel initiation (Brardinoni and Hassan, 2006; Brardinoni et al., 2009; Montgomery and Dietrich, 1992; Pirotti and Tarolli, 2010). This method gives the possibility to use an objective criterion for channel assessment. However, the extracted drainages depend on the DEM pixel size (here 25 m).

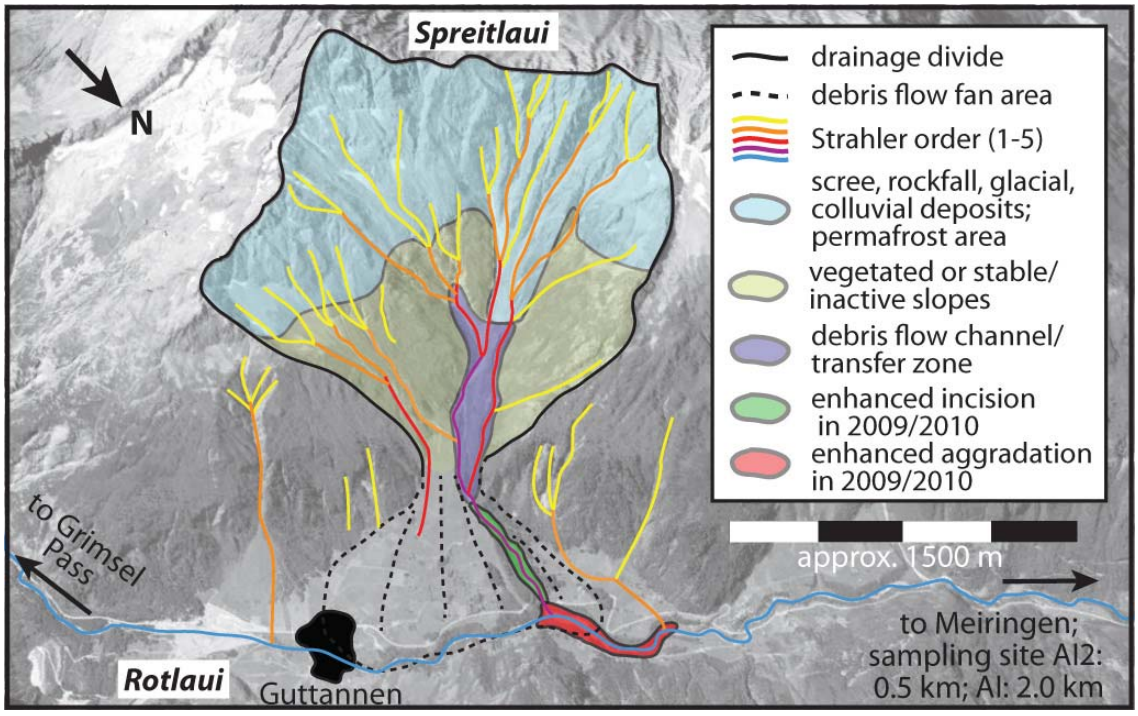

Figure DR2. Sketch of the Spreitlaui torrent showing the zones and sources that underwent erosion and aggradation during the 2009 and 2010 debris flow events.

Sample Preparation and Catchment-Wide Denudation Rate (CWDR) Calculation

Samples taken from the modern stream were sieved to a grain size of 0.1 – 1 mm, and for two samples to splits of 0.1-5 and 0.5 – 1 mm, respectively (Table 1, main text). Samples were treated with HCl to remove carbonate compounds, followed by several steps of HF-cleaning steps (Ivy-Ochs, 1996). Heavy liquid treatment removed the fractions above and below 2.62 – 2.69 g/cm^{-3}. After dissolution of the quartz, Be was separated by ion exchange chromatography using standard procedures (Ivy-Ochs, 1996), precipitated as $Be(OH)_2$ and transformed to BeO at 1000°C. The $^{10}Be/^{9}Be$ ratios of the ETH Zürich Tandem accelerator mass spectrometry (AMS) facility (Synal et al., 1997) using ETH AMS standard S555N ($^{10}Be/^{9}Be$ = 87.1x10-12 nominal) (Kubik and Christl, 2010), calibrated to standard 07KNSTD (Nishiizumi et al., 2007), with a ^{10}Be half-life of 1.387 Ma (Chmeleff et al., 2010; Korschinek et al., 2010). ^{14}C extraction and calculations follow the procedures outlined in Hippe et al. (Hippe et al., 2009; Hippe et al., 2012, sent back after revision.).

Catchment-averaged erosion rates were calculated with CosmoCalc version 1.8 (Vermeesch, 2007) with scaling to mean effective elevation and latitude according to Stone and the depth propagation of cosmic rays after (Granger and Smith, 2000). Density used was 2.5 g/cm^{-3}. Topographic shielding is 0.95. No snow shielding correction was applied. Production rates used are: total ^{10}Be – 4.67at/g/yr (Balco et al., 2008; Heisinger et al., 2002) and ^{14}C – 15.2 at/g/yr (Dugan et al., 2008).

^{10}Be Data

Table A1 Sample descprition, nuclide concentrations and denudation rates

Sample location Al: 46°22.00N, 8°13.59E, altitude 642m ; Al2: 46°41.15N, 8°14.28E, altitude 677m;
mean catchment elevation: 1904m; 10Be concentrations are reported with 1σ uncertainties.
Note that production rates are scaled using a mean production rates and are teh same for Al and Al2

Sample	date of sampling	grain size	^{10}Be conc (10^4 at/g)	^{14}C conc (10^4 at/g)	^{10}Be/^{14}C	^{10}Be denudation rate (mm/yr)	^{14}C denudation rate (mm/yr)	burial time (ky)
Al 1008	27.10.2008	0.1-1	1.51 ± 0.30	2.06 ± 0.21	0.73 ± 0.16	0.93 ± 0.19	2.59 ± 0.29	7.2 ± 2.1
Al 0409	08.04.2009	0.1-1	1.43 ± 0.24			0.98 ± 0.16		
small to medium debris-flow acitivity of 2009 and 2010								
Al 1009	07.10.2009	0.1-1	0.91 ± 0.19	3.41 ± 0.26	0.27 ± 0.06	1.55 ± 0.32	1.45 ± 0.13	0 to 2.5
Al 0310	24.03.2010	0.1-1	0.92 ± 0.20			1.53 ± 0.33		
Al 0510	23.05.2010	0.1-1	0.86 ± 0.11			1.63 ± 0.22		
Al 0610	30.06.2010	0.1-1	1.21 ± 0.11	2.34 ± 0.28	0.52 ± 0.08	1.16 ± 0.11	2.25 ± 0.34	4.7 ± 2.2
very large debris-flow acitivity of 2010								
Al 0710	06.07.2010	0.1-1	0.82 ± 0.11			1.72 ± 0.23		
Al2 0810	31.08.2010	0.1-1	0.78 ± 0.10	1.91 ± 0.29	0.41 ± 0.08	1.80 ± 0.22	2.82 ± 0.47	3.3 ± 3.0
Al2 1010	07.10.2010	0.1-1	0.84 ± 0.11			1.68 ± 0.21		
Al 1010	07.10.2010	0.1-1	1.17 ± 0.12	3.61 ± 0.24	0.32 ± 0.04	1.20 ± 0.12	1.35 ± 0.11	0 to 2.5
grain size tests								
Al 0610 L	30.06.2010	0.5-1	1.18 ± 0.14			1.19 ± 0.14		
Al 0610 S	30.06.2010	0.1-0.5	1.34 ± 0.39			1.05 ± 0.30		
Al 0810 L	31.08.2010	0.5-1	1.17 ± 0.11			1.21 ± 0.11		
Al 0810 S	31.08.2010	0.1-0.5	0.98 ± 0.10			1.44 ± 0.15		

Note that production rates (to calculate denudation rates) are scaled using a mean elevation to be comparable with other alpine data. Effective production rates would be ~7% higher.

^{14}C Data

Table A2 Summary of ^{14}C extraction steps and concentrations

for sample location see Table A1; ^{14}C concentrations are reported with 1σ uncertainties.

Sample ID	(AMS ID)	Sample mass (g)	CO_2 yield (µg)	Fraction modern $F^{14}C$[a]	$\delta^{13}C$ meas	$^{14}C/^{12}C_{abs}$ (10^{-12})[b]	^{14}C (10^4 at/g)[c]
old procedure							
AI-1008	42251.01	5.09617	39.6	0.0559 ± 0.0246	-21.02	0.0665 ± 0.0016	**2.062 ± 0.205**
AI-1009a	42436.01	5.02826	23.2	0.0586 ± 0.0322	-14.23	0.0706 ± 0.0023	2.798 ± 0.225
AI-1009c	42436.02		6.7	0.1142 ± 0.0429	-16.65	0.1371 ± 0.0059	0.610 ± 0.135
						total	**3.408 ± 0.262**
AI-1010a	42437.01	5.46562	22.0	0.0690 ± 0.0301	-17.01	0.0827 ± 0.0025	2.839 ± 0.208
AI-1010c	42437.02		5.6	0.1717 ± 0.0449	-23.11	0.2034 ± 0.0091	0.773 ± 0.128
						total	**3.612 ± 0.244**
new procedure							
AI-0610	43351.1.1	5.09322	25.0	0.0541 ± 0.0029	-16.73	0.0649 ± 0.0034	2.461 ± 0.309
AI-0610b	43351.2.1		25.1	0.0499 ± 0.0029	-16.92	0.0599 ± 0.0034	2.214 ± 0.309
						mean	**2.337 ± 0.309**
AI2-0810a	43024.1.1	5.01151	24.3	0.0509 ± 0.0030	-15.15	0.0612 ± 0.0036	1.928 ± 0.306
AI2-0810b	43024.1.2		19.4	0.0502 ± 0.0030	-15.15	0.0604 ± 0.0037	1.891 ± 0.308
						mean	**1.910 ± 0.307**

old procedure: following data aquisition outlined in Hippe et al. 2009, total value is sum from extraction and second extraction step, AI-1008 had no second extraction step

new procedure: following data aquisition outlined in Hippe et al. (in rev.), the mean results from measurement of 2 splits of the same gas

[a]Normalized to δ13C of -25‰VPDB and AD 1950

[b]Calculated after eq. 3 in Hippe et al. (in rev.).

[c]Calculated after eq. 4 in Hippe et al. (in rev.), blank corrected

For extraction procedures see (Hippe et al., 2009; Hippe et al., 2012, sent back after revision.)

Grain Size Fraction Effects on TCN-CWDR

Grain size fractions mirror catchment processes with larger grains, released by mass wasting processes, are tagged with low nuclide concentration and smaller grain sizes, representing slower hillslope processes, yielding commonly higher nuclide concentrations (Brown et al., 1998). This relationship clearly exists for a threshold grain size at around 1 mm. Below this grain size, which is the common grain size range used for CWDR studies, the picture is not as clear (Norton et al., 2011; Wittmann et al., 2007). For all samples of this study the grain size fraction of 0.1-1 mm was analyzed, while for two samples an additional split of 0.1-0.5 mm and 0.5-1 mm was analyzed (Table A1). Our test with grain size splits of 0.1 – 0.5 and 0.5 – 1 mm compared to our general grain size of 0.1 – 1 mm yielded overall homogeneity of ^{10}Be CWDR in the grain size fractions analyzed (Fig. S3).

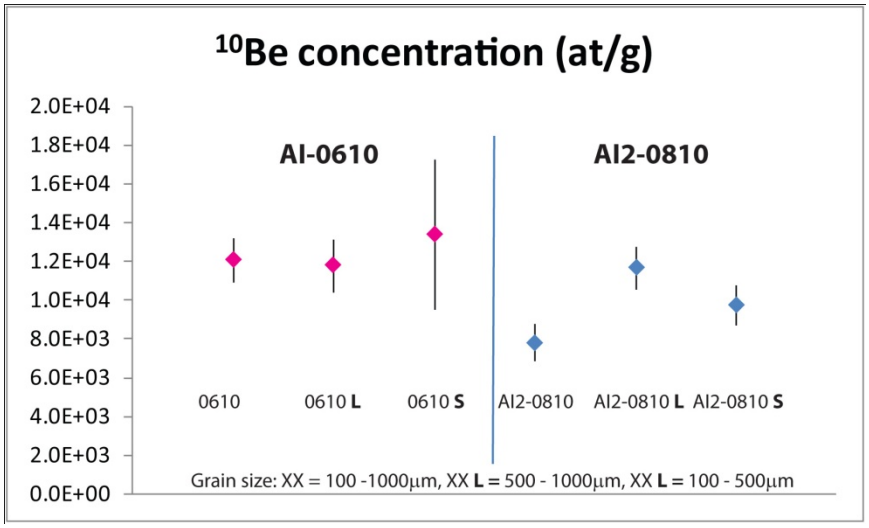

Figure DR3. ^{10}Be concentrations for grain-size splits for samples AI-0610 and AI2-0810. For denudation rates see Table 1, main text.

Comparison of Short and Long-Term Denudation Rates and Their Respective Integration Times

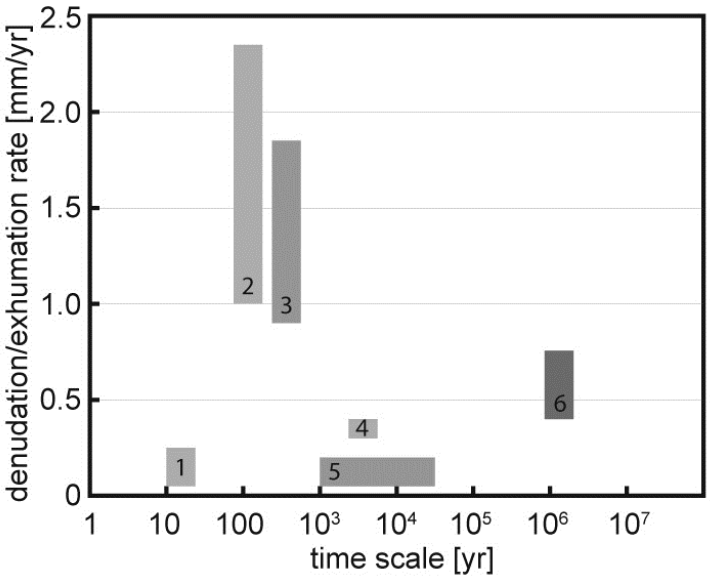

Figure DR4. Graphical presentation of the various short and long-term denudation rates and their respective integration times available from the literature in the vicinity of the Aare (see Discussion section of the main text). 1 - sediment yield (Schlunegger and Hinderer, 2003); 2 - reservoir budgets (Anselmetti et al., 2007); 3 - this study; 4 - postglacial sediment budgets/lakes (Hinderer, 2001); 5 - TCN cave studies (Haeuselmann et al., 2007); 6 - FT- data (Vernon et al., 2009).

Evaluation of Area-Weighted Mixing of Catchment-Wide Denudation Rates

In order to evaluate what nuclide concentrations will potentially be admixed from the Spreitlaui debris-flow torrent to the remaining catchment we performed a two component mixing modeling approach (Fig. S5). Hereby, published denudation rates for debris-flow areas and low order Alpine headwater catchments are taken and admixed with a background denudation rate in an area-weighted approach (A_B = 40 km^2, while the debris-flow area A_{DF} = 4 km^2). The background denudation rate is set to the denudation rates from autumn 2008/spring 2009 (mean 0.96 ± 0.18 mm/yr), and is in accordance with typical central alpine denudation rates (Wittmann et al., 2007).

Previous studies showed that debris-flow dominated or Alpine headwater catchment denudation rates range from 1 -7 mm/yr (very light grey box in (Fig. Supp. 2); see discussion and references in the main text). Mixing this range of denudation rates with the background denudation rates, the measured concentrations at site AI/AI2 (horizontal dark grey bar) after debris-flow events (mean rate mean 1.76 ± 0.22 mm/yr of AI-0610 and AI2-0810) is only possible by an area-weighted mixing, when the debris-flow dominated catchment (e.g., Spreitlaui) would contribute sediment with a denudation rates signal of >7 mm/yr (black field). In our case particularly a denudation rate of 9 mm/yr would best match this case. This denudation rate is rather at the high end of debris-flow denudation rates of low order headwater catchments reported for the Alps. By weighting of the debris-flow dominated catchment twice or three times by the area (as surrogate for supplying twice/three times as much material) the required debris-flow subcatchment denudation rates have to be in the range of 5 and 3 mm/yr, respectively, in order to yield the measured denudation rates at AI/AI2 (middle and lower panel in Fig. Supp. 2). We therefore suggest, that the likelihood is high that the debris-flow dominated catchment contributes more material than in an area-weighted approach. In fact, this is supported by field evidence where the sediment supply by the debris-flow dominated Spreitlaui torrent was dominating the entire sediment flux during 2009 and 2010 and where this sediment blocked partially the upstream sediment flux.

Note that these simple estimations ignore admixing of material from the sub-catchment downstream the entry of the debris-flow dominated catchment. This again would result in slightly lower denudation rates required from the debris-flow dominated catchment.

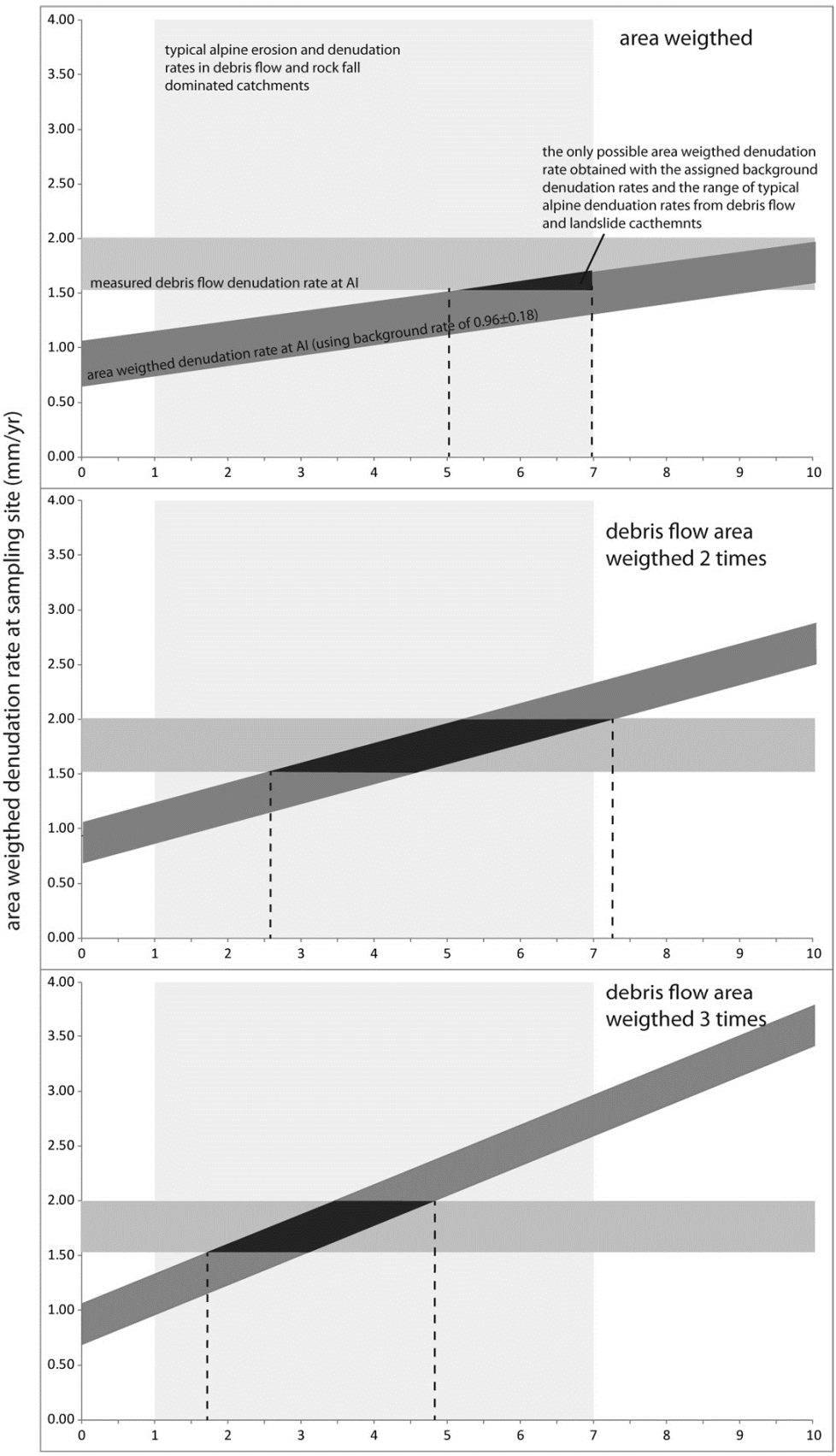
area weigthed
typical alpine erosion and denudation rates in debris flow and rock fall dominated catchments
the only possible area weigthed denudation rate obtained with the assigned background denudation rates and the range of typical alpine denduation rates from debris flow and landslide cacthemnts
measured debris flow denudation rate at AI
area weigthed denudation rate at AI (using background rate of 0.96±0.18)
debris flow area weigthed 2 times
debris flow area weigthed 3 times
area weigthed denudation rate at sampling site (mm/yr)
denudation rate from debris flow catchments (e.g., Spreitlaui)(mm/yr)

Figure DR5. Area-weighted modeling of background, perturbing and resulting mixed CWDR for the Aare-Spreitlaui setting. See text above for further information.

References

Anselmetti, F. S., Buhler, R., Finger, D., Girardclos, S., Lancini, A., Rellstab, C., and Sturm, M., 2007, Effects of Alpine hydropower dams on particle transport and lacustrine sedimentation: Aquatic Sciences, v. 69, no. 2, p. 179-198.

Balco, G., Stone, J. O., Lifton, N. A., and Dunal, T. J., 2008, A complete and easily accessible means of calculating surface exposure ages or erosion rates from Be-10 and Al-26 measurements: Quaternary Geochronology, v. 3, no. 3, p. 174-195.

Brardinoni, F., and Hassan, M. A., 2006, Glacial erosion, evolution of river long profiles, and the organization of process domains in mountain drainage basins of coastal British Columbia: Journal of Geophysical Research-Earth Surface, v. 111, no. F1, p. -.

Brardinoni, F., Hassan, M. A., Rollerson, T., and Maynard, D., 2009, Colluvial sediment dynamics in mountain drainage basins: Earth and Planetary Science Letters, v. 284, no. 3-4, p. 310-319.

Brown, E. T., Stallard, R. F., Larsen, M. C., Bourles, D. L., Raisbeck, G. M., and Yiou, F., 1998, Determination of predevelopment denudation rates of an agricultural watershed (Cayaguas River, Puerto Rico) using in-situ-produced Be-10 in river-borne quartz: Earth and Planetary Science Letters, v. 160, no. 3-4, p. 723-728.

Chmeleff, J., von Blanckenburg, F., Kossert, K., and Jakob, D., 2010, Determination of the Be-10 half-life by multicollector ICP-MS and liquid scintillation counting: Nuclear Instruments & Methods in Physics Research Section B-Beam Interactions with Materials and Atoms, v. 268, no. 2, p. 192-199.

Dugan, B., Lifton, N., and Jull, A. J. T., 2008, New production rate estimates for in situ cosmogenic C-14: Geochimica Et Cosmochimica Acta, v. 72, no. 12, p. A231-A231.

Granger, D. E., and Smith, A. L., 2000, Dating buried sediments using radioactive decay and muogenic production of Al-26 and Be-10: Nuclear Instruments & Methods in Physics Research Section B-Beam Interactions with Materials and Atoms, v. 172, p. 822-826.

Haeuselmann, P., Granger, D. E., Jeannin, P. Y., and Lauritzen, S. E., 2007, Abrupt glacial valley incision at 0.8 Ma dated from cave deposits in Switzerland: Geology, v. 35, no. 2, p. 143-146.

Heisinger, B., Lal, D., Jull, A. J., Kubik, P. W., Ivy-Ochs, S., Knie, K., and Nolte, E., 2002, Production of selected cosmogenic radionuclides by muons: 2. Capture of negative muons: Earth and Planetary Science Letters, v. 200, p. 357-369.

Hinderer, M., 2001, Late Quaternary denudation of the Alps, valley and lake fillings and modern river loads: Geodinamica Acta, v. 14, p. 231-263.

Hippe, K., Kober, F., Baur, H., Ruff, M., Wacker, L., and Wieler, R., 2009, The current performance of the in situ C-14 extraction line at ETH: Quaternary Geochronology, v. 4, no. 6, p. 493-500.

Hippe, K., Kober, F., Wacker, L., Fahrni, S. M., Ivy-Ochs, S., Akcar, N., Schluechter, C., and Wieler, R., 2012, sent back after revision., An update on cosmogenic in situ 14C analysis at ETH Zürich: Nucl. Instr. Meth. in Phys. Res.

Ivy-Ochs, S., 1996, The dating of rock surface using in situ produced ^{10}Be, ^{26}Al and ^{36}Cl, with examples from Antarctica and the Swiss AlpsPhD,11763]: ETH, 196 p.

Korschinek, G., Bergmaier, A., Faestermann, T., Gerstmann, U. C., Knie, K., Rugel, G., Wallner, A., Dillmann, I., Dollinger, G., von Gostomski, C. L., Kossert, K., Maiti, M., Poutivtsev, M., and

Remmert, A., 2010, A new value for the half-life of Be-10 by Heavy-Ion Elastic Recoil Detection and liquid scintillation counting: Nuclear Instruments & Methods in Physics Research Section B-Beam Interactions with Materials and Atoms, v. 268, no. 2, p. 187-191.

Kubik, P. W., and Christl, M., 2010, 10Be and 26Al measurements at the Zurich 6 MV Tandem AMS facility: Nuclear Instruments and Methods in Physics Research Section B: Beam Interactions with Materials and Atoms, v. 268, no. 7-8, p. 880-883.

Montgomery, D. R., and Dietrich, W. E., 1992, Channel initiation and the problem of landscape scale: Science, v. 255, p. 826-830.

Nishiizumi, K., Imamura, M., Caffee, M. W., Southon, J. R., Finkel, R. C., and McAninch, J., 2007, Absolute calibration of Be-10 AMS standards: Nucl. Instr. Meth. in Phys. Res., v. 258, no. 2, p. 403-413.

Norton, K., von Blanckenburg, F., diBase, R., Schlunegger, F., and Kubik, P. W., 2011, Cosmogenic ^{10}Be-derived denudation rates of the Eastern and Southern European Alps: Int. Jour. Earth Sciences, p. DOI 10.1007/s00531-00010-00626-y.

Pirotti, F., and Tarolli, P., 2010, Suitability of LiDAR point density and derived landform curvature maps for channel network extraction: Hydrological Processes, v. 24, no. 9, p. 1187-1197.

Schlunegger, F., and Hinderer, M., 2003, Pleistocene/Holocene climate change, re-establishment of fluvial drainage network and increase in relief in the Swiss Alps: Terra Nova, v. 15, no. 2, p. 88-95.

Synal, H.-A., Bonani, G., Doebeli, M., Ender, R. M., Gartenmann, P., Kubik, P. W., Schnabel, C., and Suter, M., 1997, Status report of the PSI/ETH AMS facility: Nuclear Instruments and Methods in Physics, no. 123, p. 62-68.

Vermeesch, P., 2007, CosmoCalc: An Excel add-in for cosmogenic nuclide calculations: Geochemistry Geophysics Geosystems, v. 8, p. Q08003, doi:08010.01029/02006GC001530.

Vernon, A. J., van der Beek, P. A., Sinclair, H. D., Persano, C., Foeken, J., and Stuart, F. M., 2009, Variable late Neogene exhumation of the central European Alps: Low-temperature thermochronology from the Aar Massif, Switzerland, and the Lepontine Dome, Italy: Tectonics, v. 28, p. Doi 10.1029/2008tc002387.

Wittmann, H., von Blanckenburg, F., Kruesmann, T., Norton, K. P., and Kubik, P. W., 2007, Relation between rock uplift and denudation from cosmogenic nuclides in river sediment in the Central Alps of Switzerland: Journal of Geophysical Research- Earth Surface, v. 112, p. F04010, doi:04010.01029/02006JF000729.